Electronic Supplementary Information

Electronic Structure Modulation of MnO_2 by Ru and F Incorporation for Efficient Proton Exchange Membrane Water Electrolysis

Dongwon Kim,[a] Anastasiia Voronova,[ab] Sol Kim,[ab] Jin Young Kim,[ab] Hee-Young Park,[a] Jong Hyun Jang,[ab] and Bora Seo[ab]*

[a] Hydrogen and Fuel Cell Research Center, Korea Institute of Science and Technology (KIST), Seoul 02792, Republic of Korea.

[b] Division of Energy & Environment Technology, KIST School, University of Science and Technology (UST), Seoul 02792, Republic of Korea.

* E-mail: brseo@kist.re.kr (B. Seo)

Contents

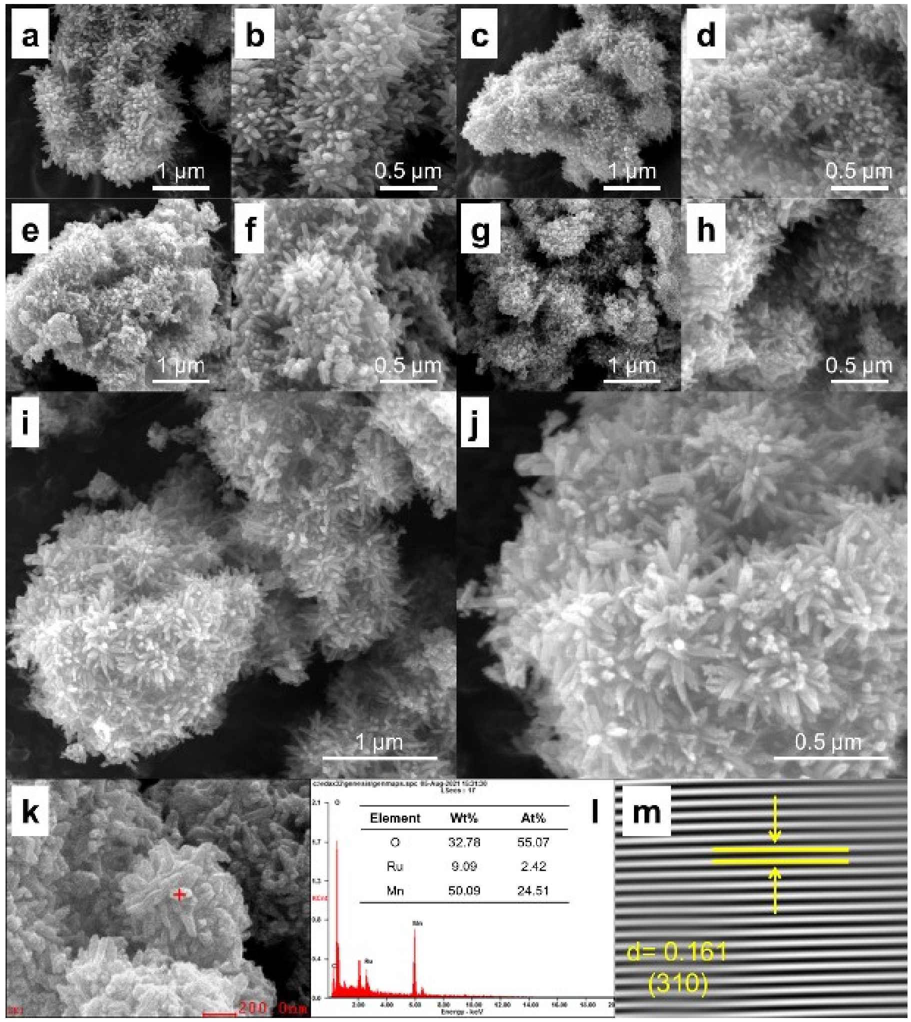

Fig. S1 SEM images of (a and b) α-MnO_2, (c and d) $(Mn_{0.94}Ru_{0.06})O_2$, (e and f) $(Mn_{0.96}Ru_{0.04})O_2$:2.5F, (g and h) $(Mn_{0.93}Ru_{0.07})O_2$:2.5F, and (i and j) $(Mn_{0.94}Ru_{0.06})O_2$:2.5F. (k and l) EDS analysis of $(Mn_{0.94}Ru_{0.06})O_2$:2.5F. (m) Inverse FFT image of $(Mn_{0.94}Ru_{0.06})O_2$:2.5F regarding (310) plane.

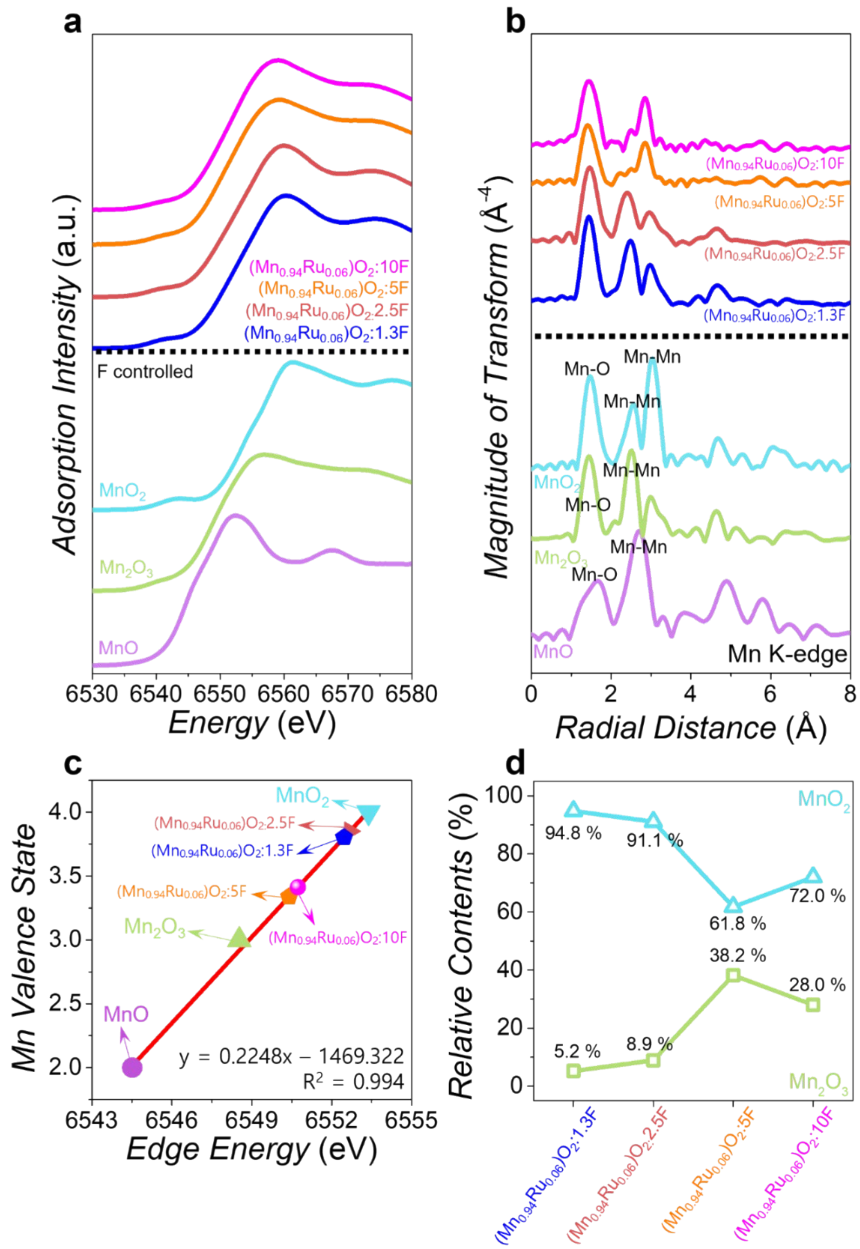

Fig. S2 (a) Mn K-edge XANES spectra of the reference materials and as-prepared samples (MnO, Mn_2O_3, α-MnO_2, $(Mn_{0.94}Ru_{0.06})O_2$:1.3F, $(Mn_{0.94}Ru_{0.06})O_2$:2.5F), $(Mn_{0.94}Ru_{0.06})O_2$:5F and $(Mn_{0.94}Ru_{0.06})O_2$:10F. (b) Radial distribution functions of the k^3-weighted EXAFS. (c) Linear regression of the edge energy in the XANES spectra and the Mn valance state. (d) Phase composition determined with LCF of the XANES spectra.

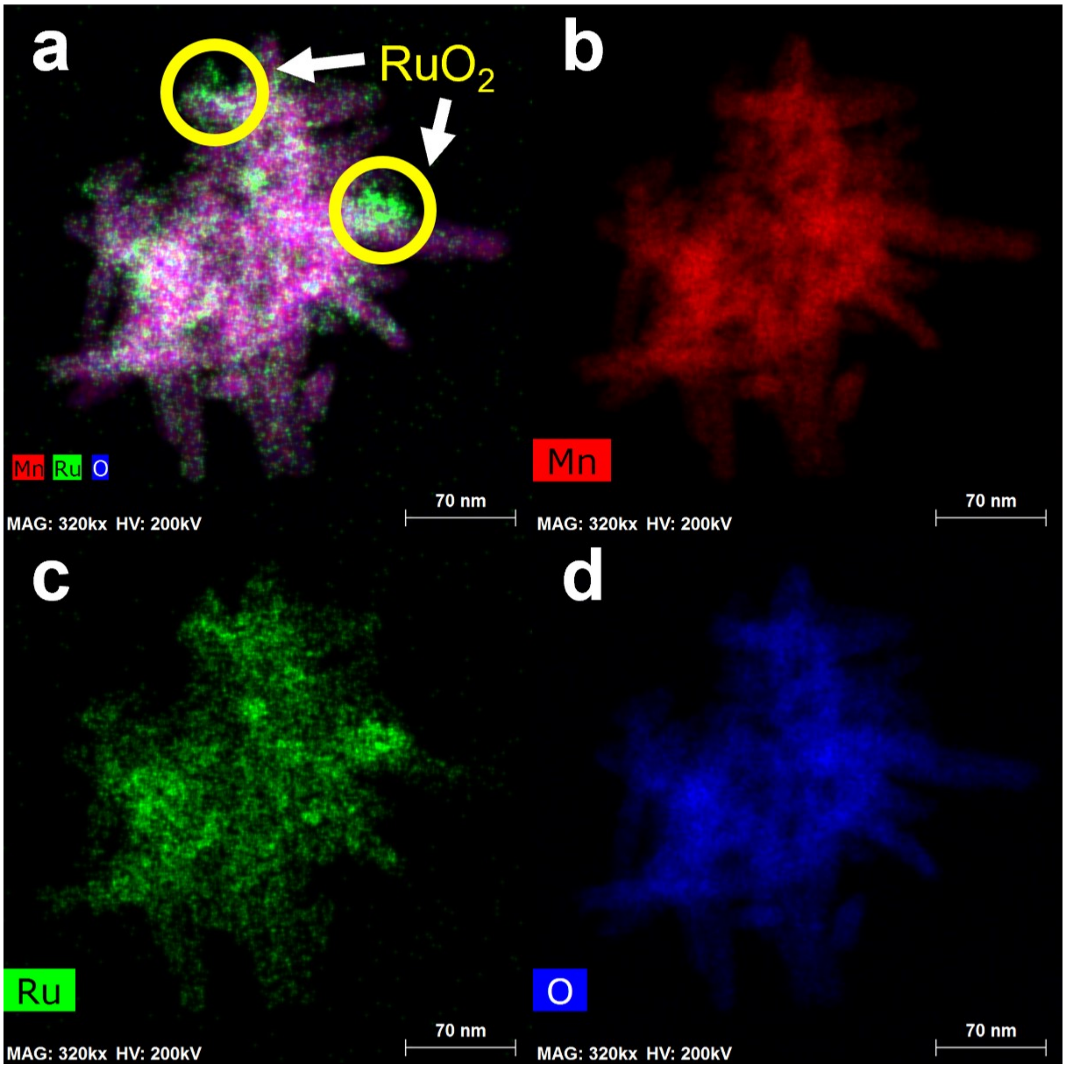

Fig. S3 EDS elemental mapping images of $(Mn_{0.93}Ru_{0.07})O_2$:2.5F; (a) overall, (b) Mn, (c) Ru and d) O.

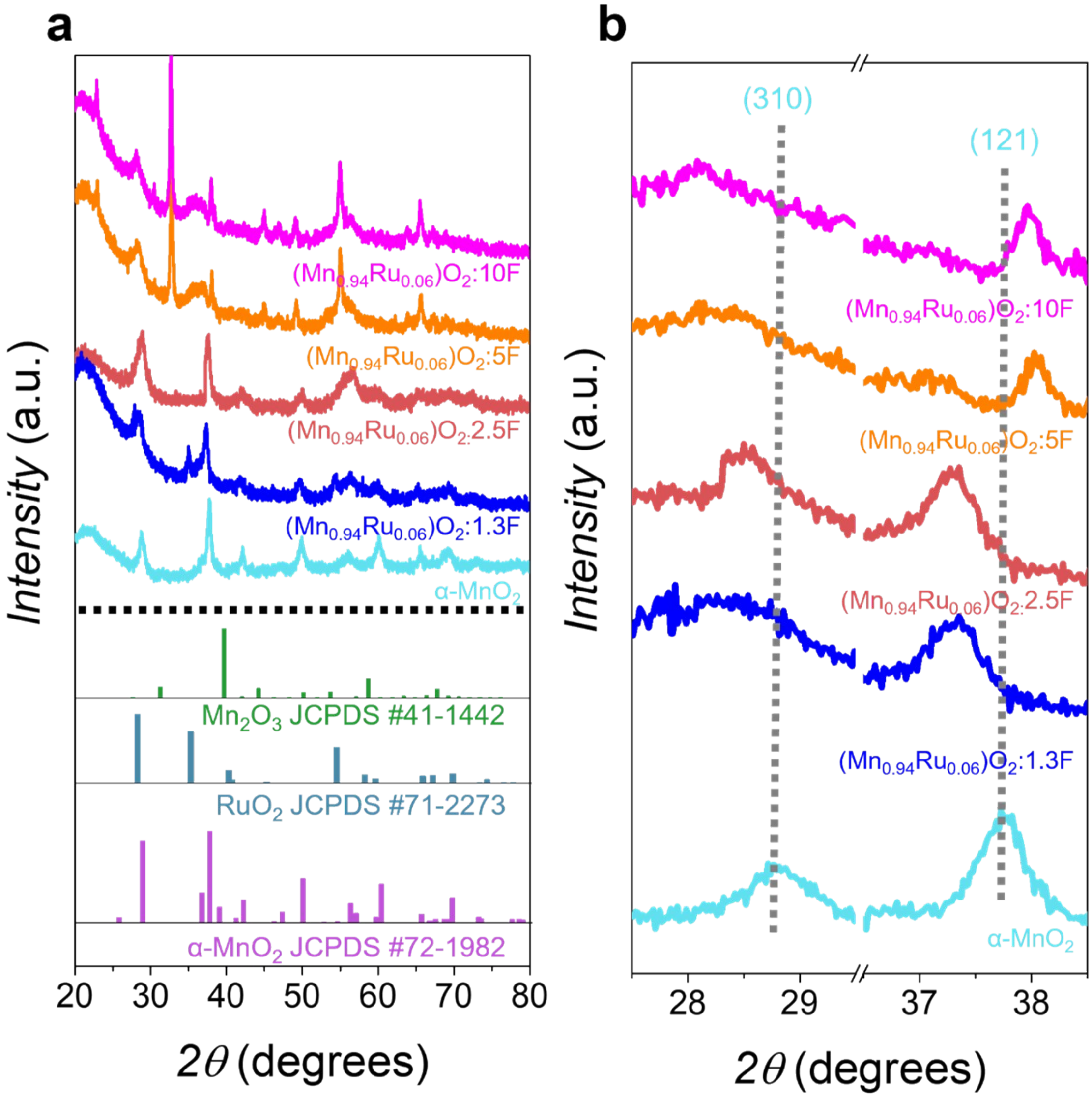

Fig. S4 (a) XRD patterns of the standard materials and as-prepared samples α-MnO_2, $(Mn_{0.94}Ru_{0.06})O_2$:1.3F, $(Mn_{0.93}Ru_{0.07})O_2$:2.5F, $(Mn_{0.94}Ru_{0.06})O_2$:5F and $(Mn_{0.94}Ru_{0.06})O_2$:10F). (b) Enlarged XRD patterns in the 2θ range of 27.5°–38.5°.

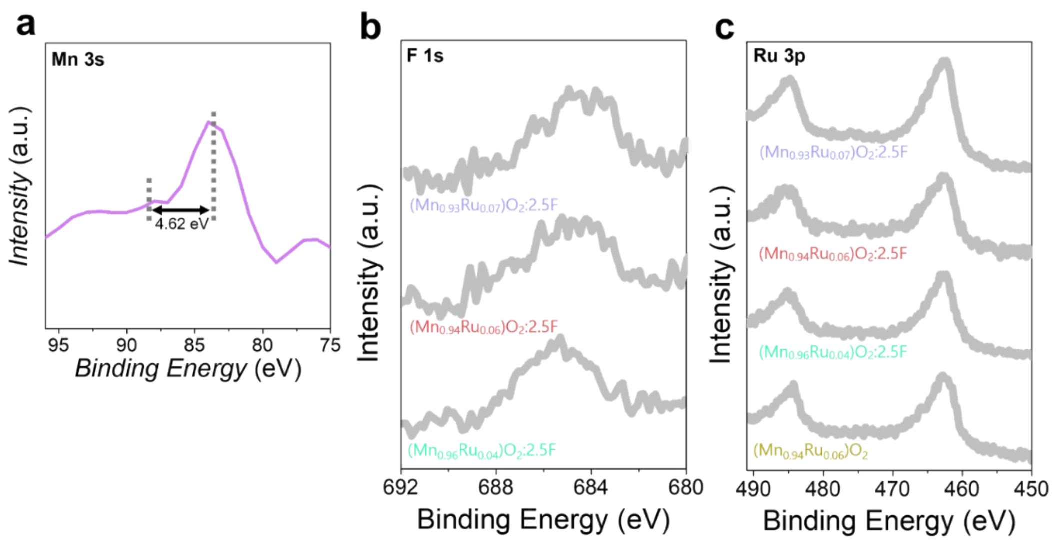

Fig. S5 (a) Mn 3s XPS spectra of $(Mn_{0.94}Ru_{0.06})O_2$:2.5F. (b) F 1s and (c) Ru 3p XPS spectra of the as-prepared samples.

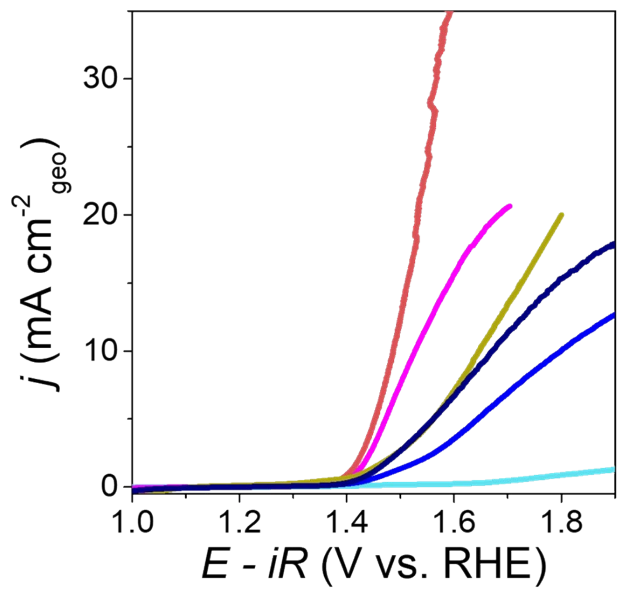

Fig. S6 LSV curves of α-MnO_2, $(Mn_{0.94}Ru_{0.06})O_2$, $(Mn_{0.94}Ru_{0.06})O_2$:1.3F, $(Mn_{0.94}Ru_{0.06})O_2$:2.5F, $(Mn_{0.94}Ru_{0.06})O_2$:5F and $(Mn_{0.94}Ru_{0.06})O_2$:10F.

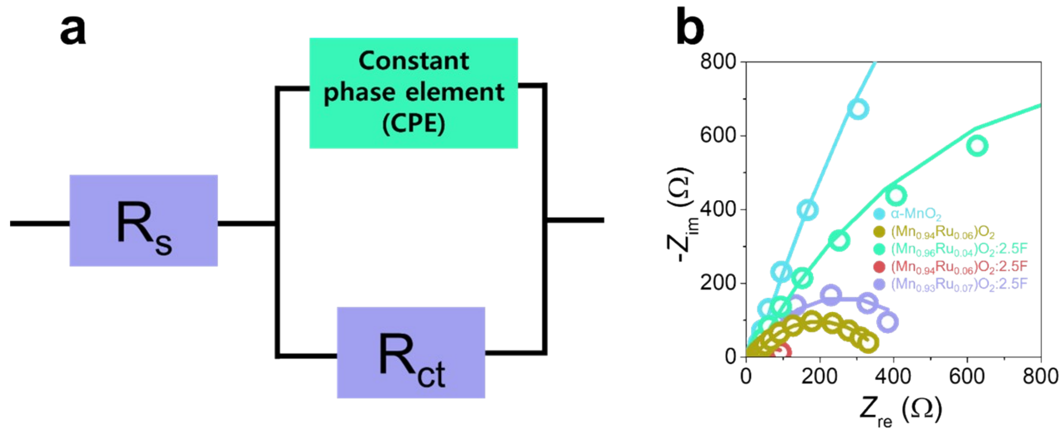

Fig. S7 (a) Equivalent circuit used for EIS fitting. (b) Nyquist plots of the as-prepared samples.

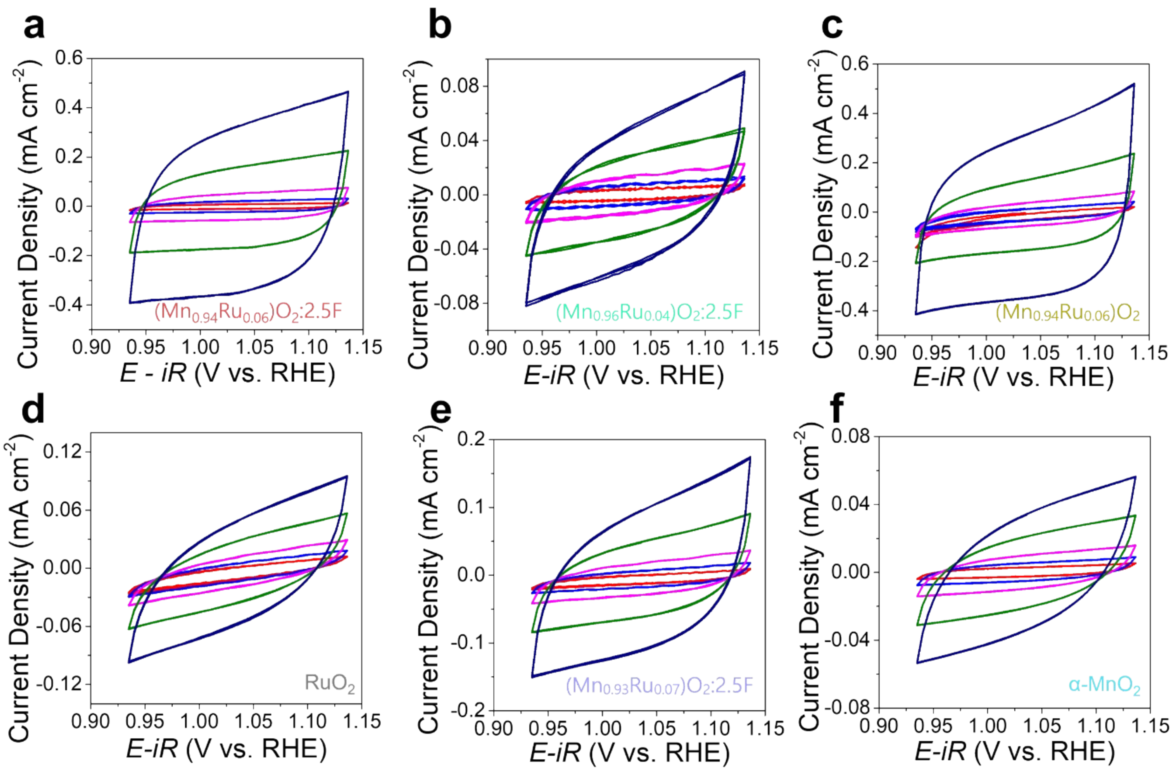

Fig. S8 The CV curves of the as-prepared samples; (a) $(Mn_{0.94}Ru_{0.06})O_2$:2.5F, (b) $(Mn_{0.96}Ru_{0.04})O_2$:2.5F, (c) $(Mn_{0.94}Ru_{0.06})O_2$, (d) RuO_2, (e) $(Mn_{0.93}Ru_{0.07})O_2$:2.5F and (f) α-MnO_2.

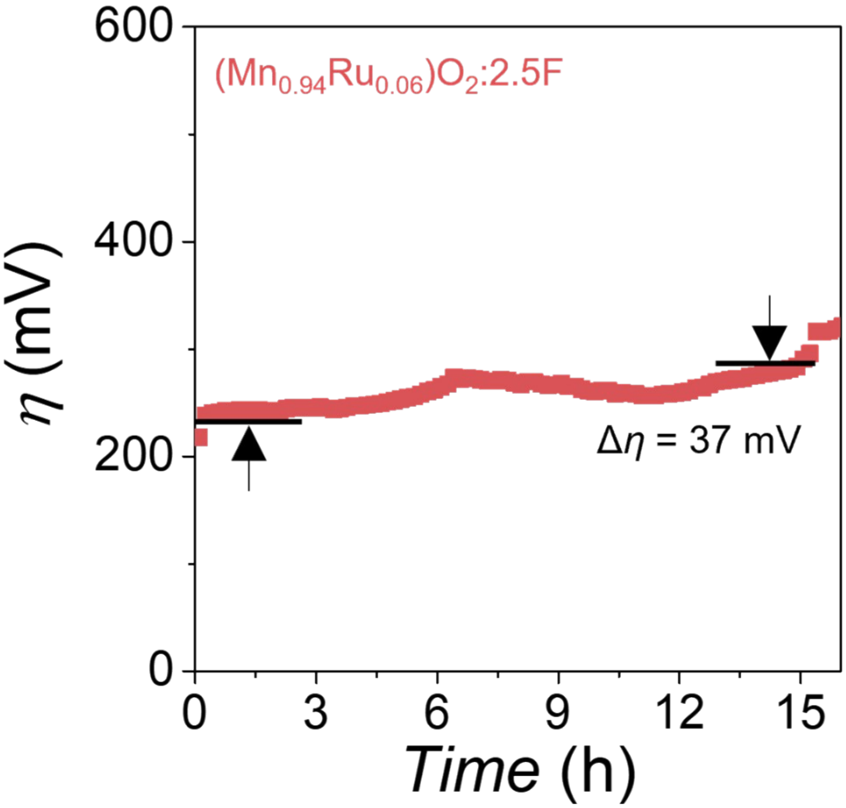

Fig. S9 Stability test of $(Mn_{0.94}Ru_{0.06})O_2$:2.5F at 10 mA cm^{-2} for 15 hours.

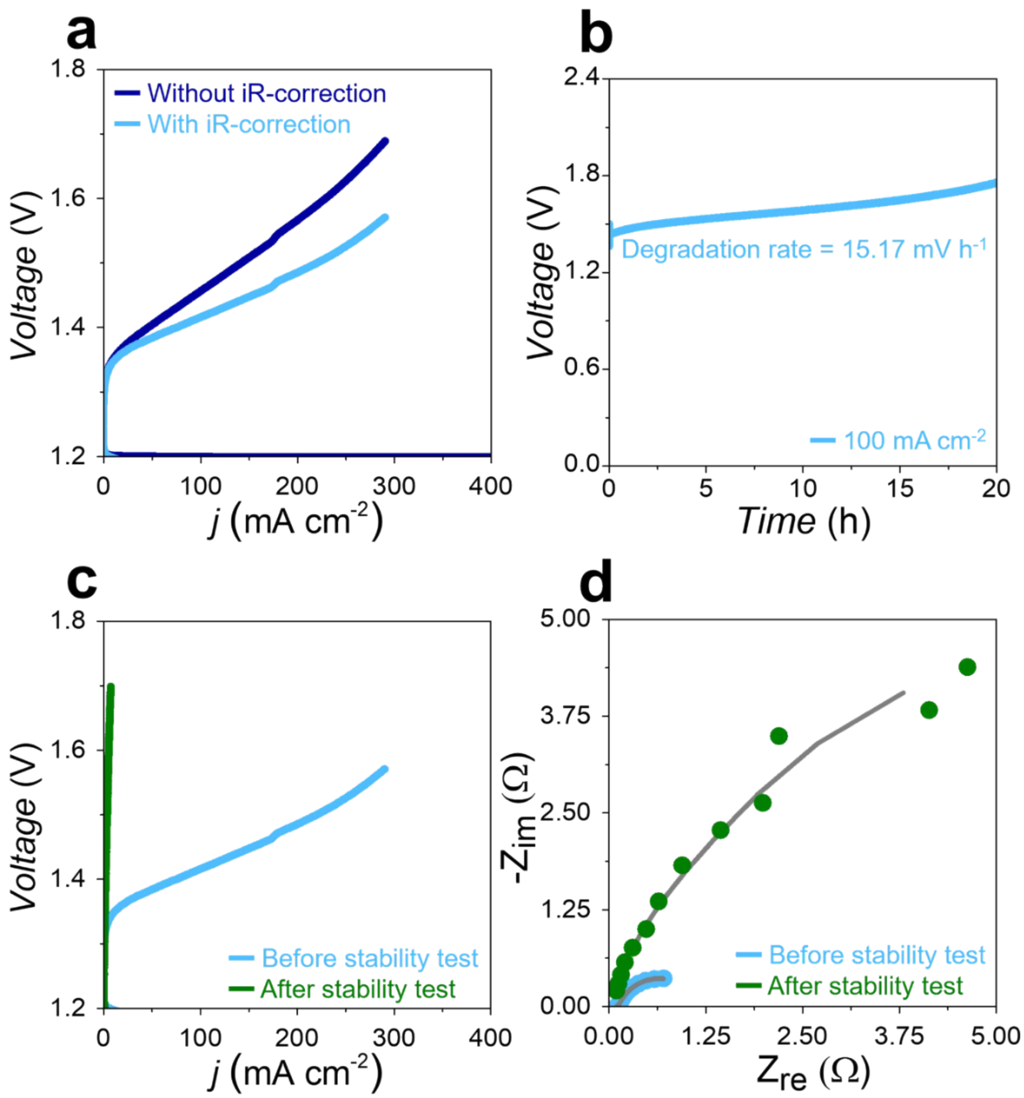

Fig. S10 The performance of the PEMWE single-cell. (a) Polarization curves of the PEMWE with $(Mn_{0.94}Ru_{0.06})O_2$:2.5F anode. (b) Stability test of the PEMWE with $(Mn_{0.94}Ru_{0.06})O_2$:2.5F anode at 100 mA cm^{-2} for 20 hours. (c) Polarization curves of $(Mn_{0.94}Ru_{0.06})O_2$:2.5F with and without iR-correction. (d) Nyquist plots of the PEMWE before and after the stability test.

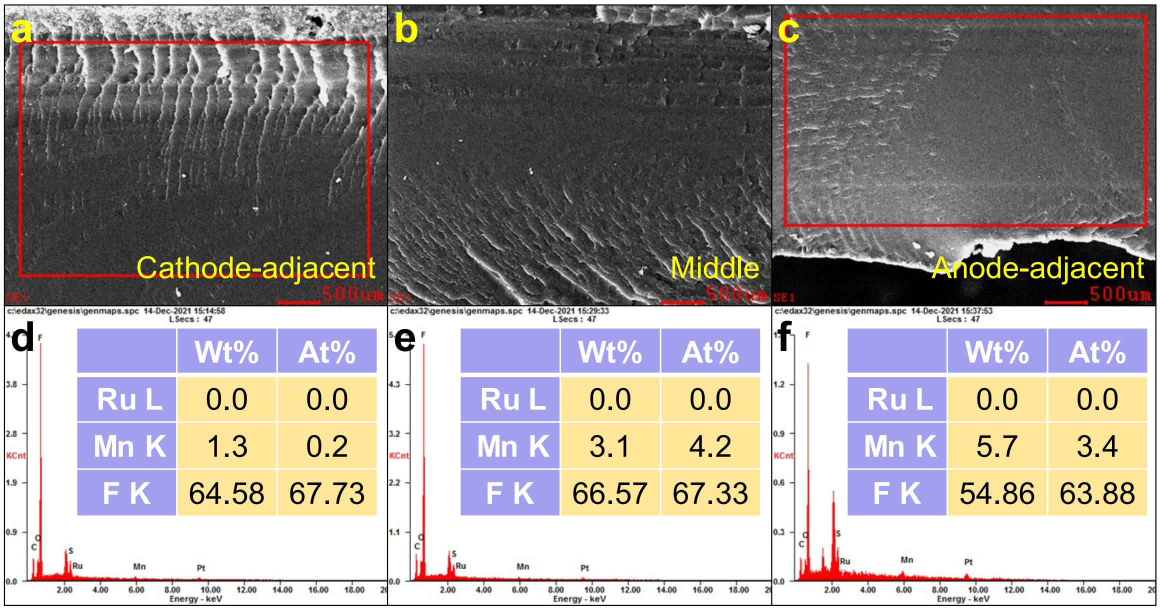

	Wt%	At%
Ru L	0.0	0.0
Mn K	1.3	0.2
F K	64.58	67.73

	Wt%	At%
Ru L	0.0	0.0
Mn K	3.1	4.2
F K	66.57	67.33

	Wt%	At%
Ru L	0.0	0.0
Mn K	5.7	3.4
F K	54.86	63.88

Fig. S11 Cross-section image of pristine MEA. (a) Cathode-adjacent, (b) middle and (c) anode-adjacent images of the MEA. The EDS results of the (d) Fig. S11a, (e) Fig. S11b and (f) Fig. S11c.

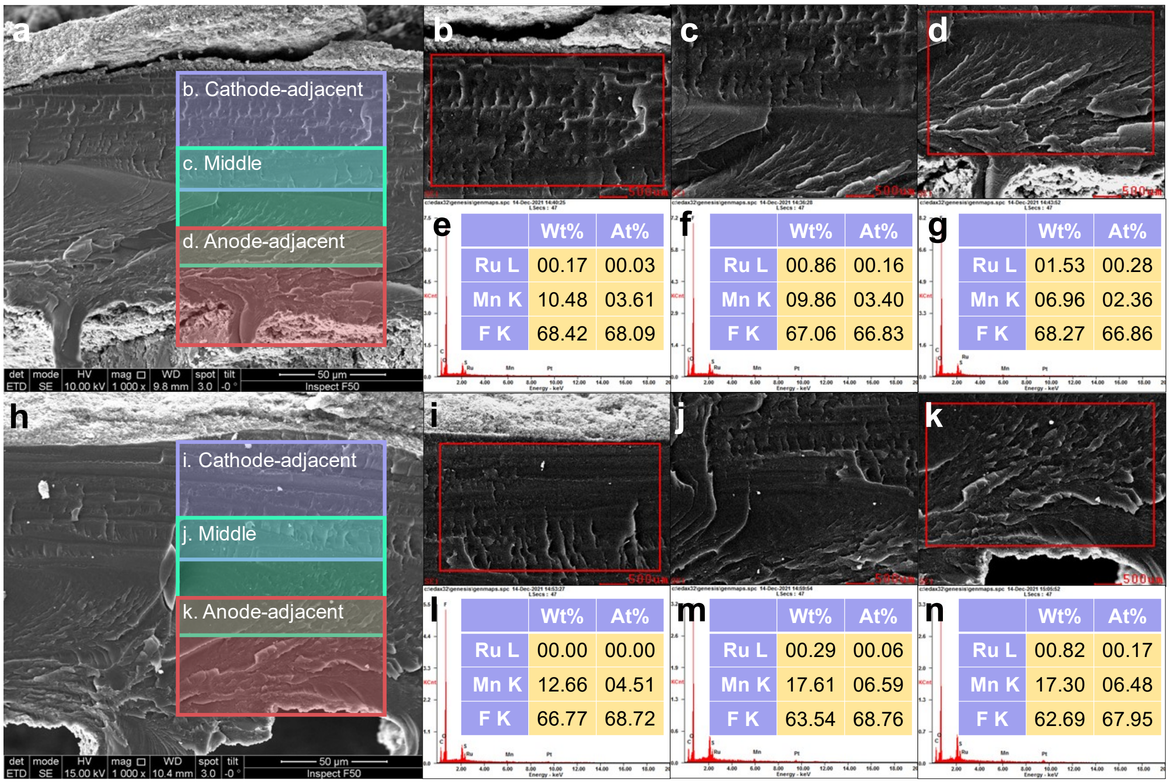

Fig. S12 (a) The cross-section image of MEA after steady-state test at 10 mA·cm^{-2} for 200 hours. The specific image of the (b) cathode-adjacent, (c) middle and (d) anode-adjacent image of MEA. The EDS results of the (e) Fig. S12b, (f) Fig. S12c and (g) Fig. S12d. (h) The image of MEA after steady-state test at 100 mA·cm^{-2} for 20 hours. The specific image of the (i) cathode-adjacent, (j) middle and (k) anode-adjacent image of MEA. The EDS results of the (l) Fig. S12i, (m) Fig. S12j and (n) Fig. S12k.

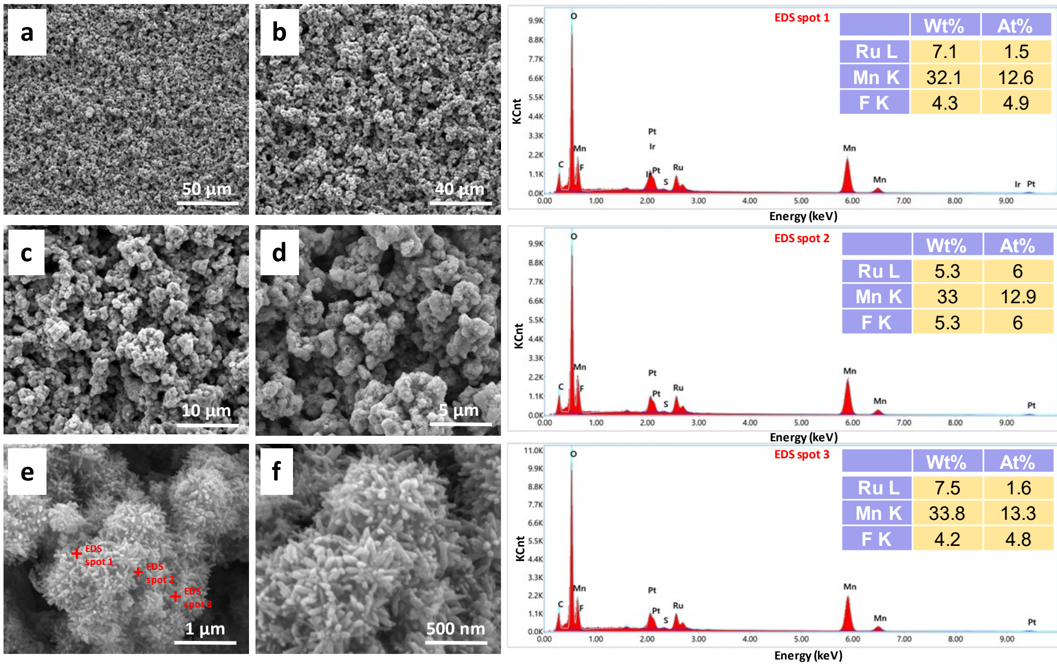

Fig. S13 Surface SEM/EDS analyses of the pristine $(Mn_{0.94}Ru_{0.06})O_2$:2.5F on membrane.

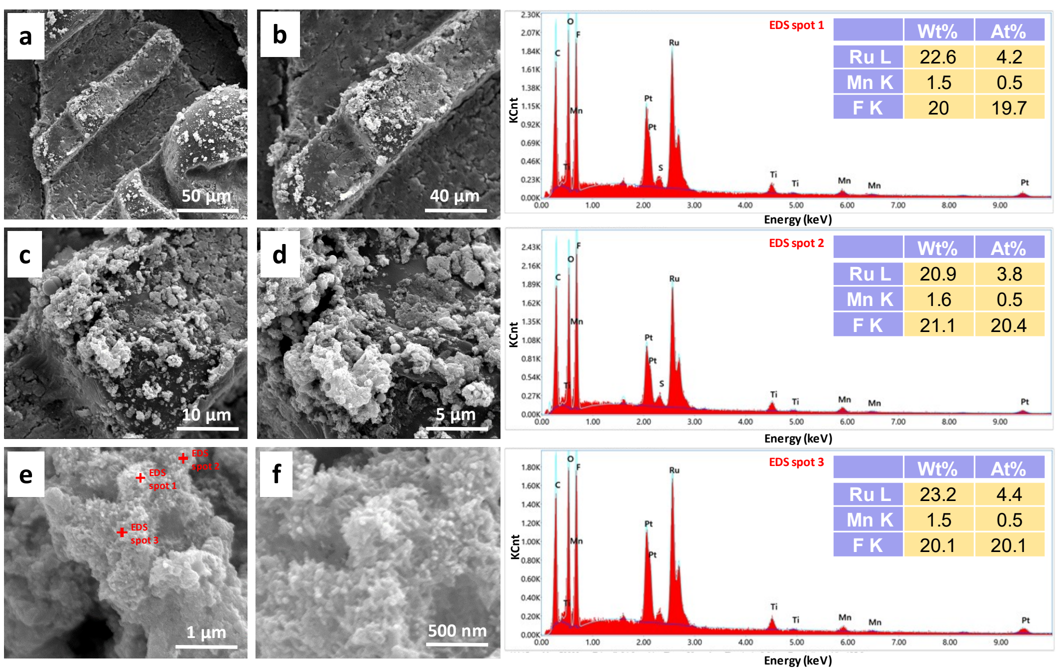

Fig. S14 Surface SEM/EDS analyses of the $(Mn_{0.94}Ru_{0.06})O_2$:2.5F after steady-state test at 10 mA·cm^{-2} for 200 hours.

Table S1. Contents of Mn and Ru determined by the quantitative EDS analysis.

	Atomic percentage		Weight percentage	
Samples	**Mn (at %)**	**Ru (at %)**	**Mn (wt %)**	**Ru (wt %)**
$(Mn_{0.94}Ru_{0.06})O_2$	30.97	2.38	56.56	8.00
$(Mn_{0.96}Ru_{0.04})O_2$:2.5F	32.29	1.53	59.38	5.18
$(Mn_{0.94}Ru_{0.06})O_2$:2.5F	31.52	2.29	57.22	7.65
$(Mn_{0.93}Ru_{0.07})O_2$:2.5F	30.76	3.71	54.28	12.04

Table S2 Edge energies and oxidation states determined by the Mn K-edge XANES spectra.

Samples	Edge energy (eV)	Oxidation state
MnO	6544.51	2+
Mn_2O_3	6548.53	3+
α-MnO_2	6553.38	4+
$(Mn_{0.96}Ru_{0.04})O_2$:2.5F	6552.85	3.89+
$(Mn_{0.94}Ru_{0.06})O_2$:2.5F	6552.68	3.85+
$(Mn_{0.93}Ru_{0.07})O_2$:2.5F	6553.01	3.92+
$(Mn_{0.94}Ru_{0.06})O_2$	6553.31	3.99+
$(Mn_{0.94}Ru_{0.06})O_2$:1.3F	6552.46	3.80+
$(Mn_{0.94}Ru_{0.06})O_2$:5F	6550.40	3.34+
$(Mn_{0.94}Ru_{0.06})O_2$:10F	6550.73	3.41+

Table S3 Phase composition determined by the LCF of the Mn K-edge XANES spectra.

Samples	MnO	Mn_2O_3	MnO_2
$(Mn_{0.96}Ru_{0.04})O_2$:2.5F	0.000	0.042	0.958
$(Mn_{0.94}Ru_{0.06})O_2$:2.5F	0.000	0.089	0.911
$(Mn_{0.93}Ru_{0.07})O_2$:2.5F	0.000	0.030	0.970
$(Mn_{0.94}Ru_{0.06})O_2$	0.000	0.004	0.996
$(Mn_{0.94}Ru_{0.06})O_2$:1.3F	0.000	0.052	0.948
$(Mn_{0.94}Ru_{0.06})O_2$:5F	0.000	0.382	0.618
$(Mn_{0.94}Ru_{0.06})O_2$:10F	0.000	0.280	0.720

Table S4 Shifts in the XRD peak positions for (310) and (121) planes from those of the α-MnO_2.

Sample	2θ for (310) (degrees)	Δ2θ (degrees)	2θ for (121) (degrees)	Δ2θ (degrees)
α-MnO_2	28.70	0	37.76	0
$(Mn_{0.94}Ru_{0.06})O_2$	28.57	−0.13	37.59	−0.17
$(Mn_{0.96}Ru_{0.04})O_2$:2.5F	28.52	−0.18	37.44	−0.32
$(Mn_{0.94}Ru_{0.06})O_2$:2.5F	28.40	−0.3	37.28	−0.48
$(Mn_{0.93}Ru_{0.07})O_2$:2.5F	28.38	−0.32	37.37	−0.39

Table S5 XRD peak positions, FWHMs, crystallite sizes and d-spacing values for the (121) plane, determined by Scherrer analysis.

Sample	2θ for (121) (degrees)	θ (degrees)	FWHM	Crystallite size (nm)	d-spacing (nm)
α-MnO_2	37.75	18.87	0.522	16	0.238
$(Mn_{0.94}Ru_{0.06})O_2$	37.59	18.79	0.517	16	0.239
$(Mn_{0.96}Ru_{0.04})O_2$:2.5F	37.44	18.72	0.510	16	0.240
$(Mn_{0.94}Ru_{0.06})O_2$:2.5F	37.28	18.64	0.513	16	0.241
$(Mn_{0.93}Ru_{0.07})O_2$:2.5F	37.37	18.68	0.513	16	0.241

Table S6 XPS peak position determined from deconvolution of Mn 2p XPS spectra.

Samples	Peak position			
	Mn 2p$_{3/2}$ (eV)	**Mn 2p$_{1/2}$ (eV)**	**Mn 2p$_{3/2}$ (eV)**	**Mn 2p$_{1/2}$ (eV)**
α-MnO_2	642.8	654.5	641.6	653.4
$(Mn_{0.94}Ru_{0.06})O_2$	642.8	653.6	640.9	652.6
$(Mn_{0.96}Ru_{0.04})O_2$:2.5F	642.6	653.9	641.3	652.9
$(Mn_{0.94}Ru_{0.06})O_2$:2.5F	642.6	653.9	641.3	652.9
$(Mn_{0.93}Ru_{0.07})O_2$:2.5F	642.4	653.7	641.1	652.7

Table S7 XPS peak position determined from the deconvolution of O 1s XPS spectra.

Samples	O 1s (eV)		
	Lattice oxygen	**Oxygen vacancy**	**Adsorbed water**
α-MnO_2	529.7	531.3	533.0
$(Mn_{0.94}Ru_{0.06})O_2$	529.0	530.5	531.9
$(Mn_{0.96}Ru_{0.04})O_2$:2.5F	529.2	530.8	532.8
$(Mn_{0.94}Ru_{0.06})O_2$:2.5F	529.0	530.6	532.6
$(Mn_{0.93}Ru_{0.07})O_2$:2.5F	529.0	530.7	532.6

Table S8 XPS peak area ratio of Mn^{3+}/Mn^{4+} and O_V/O_L determined by the deconvolution of XPS spectra.

Samples	Mn^{3+}/Mn^{4+}	O_V/O_L
α-MnO_2	0.586	0.558
$(Mn_{0.94}Ru_{0.06})O_2$	0.529	0.472
$(Mn_{0.96}Ru_{0.04})O_2$:2.5F	0.819	0.706
$(Mn_{0.94}Ru_{0.06})O_2$:2.5F	0.936	0.806
$(Mn_{0.93}Ru_{0.07})O_2$:2.5F	0.919	0.730

Table S9 XPS peak positions for F 1s and Ru 3p XPS spectra.

Samples	F 1s (eV)	Ru^{4+}		Ru^{0}	
		Ru $3p_{3/2}$ (eV)	Ru $3p_{1/2}$ (eV)	Ru $3p_{3/2}$ (eV)	Ru $3p_{1/2}$ (eV)
$(Mn_{0.94}Ru_{0.06})O_2$	-	463.7	485.9	461.9	484.1
$(Mn_{0.96}Ru_{0.04})O_2$:2.5F	685.4	463.7	485.9	461.9	484.1
$(Mn_{0.94}Ru_{0.06})O_2$:2.5F	685.0	463.7	485.9	461.9	484.1
$(Mn_{0.93}Ru_{0.07})O_2$:2.5F	684.6	463.7	485.9	461.9	484.1

Table S10 Series and charge transfer resistances obtained from the EIS analysis.

Samples	R_s (Ω)	R_{ct} (Ω)
α-MnO_2	23.7	10126
$(Mn_{0.94}Ru_{0.06})O_2$	31.9	346
$(Mn_{0.96}Ru_{0.04})O_2$:2.5F	22.7	7799
$(Mn_{0.94}Ru_{0.06})O_2$:2.5F	30.0	86
$(Mn_{0.93}Ru_{0.07})O_2$:2.5F	22.5	460

Table S11 OER activity in terms of overpotential at 10 mA·cm^{-2}, Tafel slopes, C_{dl}, and ECSA.

Samples	η at 10 mA cm^{-2} (mV)	Tafel slope (mV dec^{-1})	C_{dl} (mF)	ECSA (cm^2)
α-MnO_2	n.a.	364	0.07	2.0
$(Mn_{0.94}Ru_{0.06})O_2$	421	97	0.65	18.6
$(Mn_{0.96}Ru_{0.04})O_2$:2.5F	766	133	0.10	2.9
$(Mn_{0.94}Ru_{0.06})O_2$:2.5F	257	62	0.66	18.9
$(Mn_{0.93}Ru_{0.07})O_2$:2.5F	642	99	0.19	5.4

Table S12 OER activity comparison of Mn and noble-metal-based catalysts in terms of loading, overpotential at 10 mA·cm^{-2} and mass activity.

Samples	Loading (mg cm^{-2})	Noble metal loading (mg cm^{-2})	η (mV)	Mass activity (mA mg^{-1})	Reference
$(Mn_{0.7}Ir_{0.3})O_2$:10F	0.3	0.135	245	74.06	[S1]
$(Mn_{0.8}Ir_{0.2})O_2$:10F	0.3	0.101	200	99.18	[S1]
$(Mn_{0.8}Nb_{0.2})O_2$:10F	0.3	0.059	680	169.60	[S2]
$Ir_{0.4}/Mn_{0.6}$	0.2	0.108	237	92.24	[S3]
$RuO_2/(Co,Mn)_3O_4$	n.a.	0.06	270	166.67	[S4]
Ir-MnO_2	4	0.205	218	48.73	[S5]
Mn-RuO_2	0.275	0.196	158	50.93	[S6]
12Ru/MnO_2	0.2	0.023	161	434.8	[S7]
This work	0.216	0.017	250	588.24	This work

Table S13 Contents of Mn and Ru in electrolyte after stability test, determined by the ICP-MS analysis.

Sample	Mn (ppm)	Ru (ppm)
$(Mn_{0.94}Ru_{0.06})O_2$:2.5F	3.157	0.053

Table S14 Contents of Mn, Ru and F in membrane after stability test at 10 mA cm^{-2} and 100 mA cm^{-2}.

MEA sector	10 mA cm^{-2}			100 mA cm^{-2}		
	Mn (at%)	Ru (at%)	F (at%)	Mn (at%)	Ru (at%)	F (at%)
Cathode-adjacent	3.61	0.03	68.09	4.51	0.00	68.72
Middle	3.40	0.16	66.83	6.59	0.06	68.76
Anode-adjacent	2.36	0.28	66.86	6.48	0.17	67.95

Table S15 Relative contents of Mn, Ru and F in catalyst layer before the stability test at 10 mA cm^{-2} (normalized data considering only Mn, Ru and F).

MEA sector	10 mA cm^{-2}		
	Mn (at%)	**Ru (at%)**	**F (at%)**
Point 1	66.3	7.9	25.8
Point 2	62.9	7.8	29.3
Point 3	67.5	8.1	24.4
Average	65.6	7.8	26.5

Table S16 Relative contents of Mn, Ru and F in catalyst layer after stability test at 10 mA cm^{-2} (normalized data considering only Mn, Ru and F).

MEA sector	10 mA cm^{-2}		
	Mn (at%)	**Ru (at%)**	**F (at%)**
Point 1	2.0	17.2	80.7
Point 2	2.0	15.4	82.6
Point 3	2.0	17.6	80.4
Average	2.0	16.7	81.2

References

[S1] S. D. Ghadge, P. P. Patel, M. K. Datta, O. I. Velikokhatnyi, R. Kuruba, P. M. Shanthi and P. N. Kumta, *RSC Adv.*, 2017, **7**, 17311–17324.

[S2] S. D. Ghadge, O. I. Velikokhatnyi, M. K. Datta, P. M. Shanthi, S. Tan and P. N. Kumta, *ACS Appl. Energy Mater.*, 2020, **3**, 541–557.

[S3] S. Chen, H. Huang, P. Jiang, K. Yang, J. Diao, S. Gong, S. Liu, M. Huang, H. Wang and Q. Chen, *ACS Catal.*, 2020, **10**, 1152–1160.

[S4] S. Niu, X.-P. Kong, S. Li, Y. Zhang, J. Wu, W. Zhao and P. Xu, *Appl. Catal., B*, 2021, **297**, 120442.

[S5] Z. Shi, Y. Wang, J. Li, X. Wang, Y. Wang, Y. Li, W. Xu, Z. Jiang, C. Liu, W. Xing and J. Ge, *Joule*, 2021, **5**, 2164–2176.

[S6] S. Chen, H. Huang, P. Jiang, K. Yang, J. Diao, S. Gong, S. Liu, M. Huang, H. Wang and Q. Chen, *ACS Catal.*, 2020, **10**, 1152–1160.

[S7] C. Lin, J.-L. Li, X. Li, S. Yang, W. Luo, Y. Zhang, S.-H. Kim, D.-H. Kim, S. S. Shinde, Y.-F. Li, Z.-P. Liu, Z. Jiang and J.-H. Lee, *Nat. Catal.*, 2021, **4**, 1012–1023.